BER the international journal of bridge engineering management and research

Assessing Damage Behavior of Reinforced Concrete Bridge Piers under Low-Velocity Car Crashes: Experimental and Numerical Study

Suman Roy*

Submitted: 12 April 2026 **Accepted:** 24 June 2026 **Publication date:** 10 July 2026

DOI: 10.70465/ber.v3i3.90

Abstract: Vehicle collisions subject reinforced concrete (RC) bridge piers to high strain-rate dynamic loads, producing complex material interactions and an apparent strength enhancement commonly quantified by the dynamic increase factor (DIF). During impact, the concrete cover, acting as a sacrificial layer, experiences initial damage due to the car crash, subsequently transferring forces to the transverse reinforcement and altering the pier's axial and flexural behavior. This study presents an experimental investigation of low-velocity vehicular collisions involving subcompact and sedan cars, with emphasis on cosmetic surface damage and global structural response. Finite element simulations developed in ANSYS are employed to reproduce the experimental behavior and to validate estimates of post-impact residual capacity. Damage levels are further quantified using a combined probabilistic and reliability-based framework to assess the likelihood and severity of cosmetic damage. The results offer valuable insights into impact-induced damage mechanisms, enable rational evaluation of residual structural capacity, and support informed decisions regarding repair or strengthening. Additionally, chaotic analysis has been further scrutinized in terms of chaotic risk amplification factor (CRAF) to reinforce the findings. This present study contributes to forensic assessments of RC bridge piers' serviceability and resilience following vehicular impact events.

Author keywords: Representative prototype RC bridge piers; low-velocity car crashes; Finite Element (FE) simulations; determination of cosmetic damage; validation of experimental results; and validation of experimental results

Introduction

Bridge piers are subjected to highly dynamic actions arising from seismic events, blasts, and vehicular collisions. These actions may induce damage ranging from superficial surface deterioration to severe structural degradation, potentially leading to collapse. While the seismic performance of reinforced concrete (RC) piers has been extensively investigated, the effects of low-velocity vehicular impacts, particularly those resulting in minor or cosmetic damage, remain inadequately understood.

In practice, RC piers experiencing low-velocity vehicular collisions are often left unrepaired because the observed damage is perceived as non-structural. However, even minor impact-induced damage may compromise stiffness, alter load paths, and reduce residual capacity over time. At present, there is no reliable framework for quantifying capacity degradation associated with such damage, raising concerns regarding the safety and serviceability of impacted piers when subjected to subsequent loading, including earthquakes, blasts, or additional collisions. This deficiency highlights the need for systematic investigation into the cumulative effects of cosmetic damage and its potential role in progressive or catastrophic failure.

Existing design codes provide limited guidance for RC piers subjected to high strain-rate loading and are particularly inadequate in addressing post-impact deformation and residual capacity following low-severity vehicular collisions. Although dynamic impact scenarios, including vehicle crashes and blast loading, have been studied, the specific response of RC bridge piers under low-velocity vehicular impacts remains largely unexplored. This limitation is critical given that vehicular collisions represent one of the most frequent impact hazards for bridge substructures, a risk amplified by increasing traffic volumes.[1]

This study addresses the identified knowledge gap by investigating the structural performance of RC bridge piers subjected to low-velocity vehicular impact. The objectives are to characterize cosmetic damage, identify dominant failure mechanisms, and quantify residual load-carrying capacity. An experimental program consisting of pendulum impact tests on four half-scale RC pier specimens was conducted to simulate realistic low-speed vehicle collisions. The

*Corresponding Author: Suman Roy.
Email: sumanroy74@gmail.com
Department of Civil and Environmental Engineering, Utah State University, Logan, Utah 84322 U.S.A

Discussion period open till six months from the publication date. Please submit separate discussion for each individual paper. This paper is a part of the Vol. 3 of the International Journal of Bridge Engineering, Management and Research (© BER), ISSN 3065-0569.

experimental results provide insight into damage evolution, energy dissipation, and post-impact serviceability.

Previous studies have identified shear failure and overturning moments at the column base as dominant failure modes in RC columns subjected to impact loading.[2,3] Investigations involving sequential loading scenarios, such as blast followed by vehicular impact, have further demonstrated the influence of column diameter, longitudinal reinforcement ratio, and transverse reinforcement on structural reliability.[4] Increasing column stiffness and modifying pier geometry have been proposed as effective strategies to enhance resistance to low-velocity dynamic impacts through improved energy dissipation.[5]

Despite these advances, the influence of cosmetic damage caused by low-velocity vehicular impacts on residual capacity remains largely unquantified. To address this gap, experimental findings are used to define post-impact performance levels, which are subsequently validated and extended through finite element modeling (FEM). The numerical models simulate quasi-static low-speed impact conditions, enabling replication of realistic vehicle–pier interaction and identification of critical failure mechanisms. Stress concentration and plastic hinge formation are consistently observed near the column–foundation interface, which governs energy dissipation through crack initiation and propagation.[6]

To replicate in-service conditions, axial preloading was applied to the pier specimens prior to impact, and corresponding FEM simulations were developed for numerical validation. The interaction between axial compression and lateral impact forces was analyzed to characterize stress, strain, and deformation behavior in the vicinity of the column base. Uniaxial material constitutive models have been adopted to capture localized damage with sufficient accuracy, supporting a comprehensive assessment of post-impact structural performance.

Furthermore, the circular geometry of RC piers, commonly adopted to enhance short-duration impact performance, has been re-examined in the context of vehicular collision loading.[7] Detailed assessment of cosmetic damage at both material and member levels has been employed to evaluate complex existing load-transfer mechanisms and identify key considerations for post-impact inspection and decision-making prior to returning piers to service.[8]

A key contribution of this research is the integrated experimental–numerical framework developed to investigate the nonlinear response of RC bridge piers subjected to low-velocity vehicular impacts. Realistic crash scenarios based on Class-I vehicle parameters are considered to quantify residual capacity following impact. In addition, probabilistic reliability analyses are conducted to account for uncertainties associated with damage progression and failure risk, providing a rational basis for post-impact assessment and design recommendations.

The findings offer critical insights into low-velocity impact behavior, addressing current gaps in design provisions and highlighting the need for revised evaluation criteria. Through detailed parametric and push-over analyses, this study informs future efforts to develop robust assessment methods and enhance the safety and longevity of bridge infrastructure. In conclusion, this research provides a foundational framework for understanding and assessing the post-impact performance of RC bridge piers as follows:

- This study presents a comprehensive investigation into the post-impact performance of RC bridge piers subjected to short-duration, low-velocity vehicular collisions. Such impacts, though often considered minor, can cause significant cosmetic and structural damage that compromises long-term performance. By examining damage propagation, energy dissipation, and changes in load-bearing behavior, the study seeks to better understand the implications of seemingly low-severity collisions on the structural integrity and residual capacity of bridge piers.
- To strengthen and validate the experimental findings, a series of detailed FEM simulations were performed. These simulations closely replicate the experimental conditions with trivial deviation and provide deeper insights into failure mechanisms, such as shear cracking, localized plastic deformation, and stress redistribution. The numerical analyses serve not only to confirm the experimental observations but also to extend the investigation to a broader range of impact scenarios and structural configurations.
- Recognizing the need for practical assessment tools, the study also incorporates reliability-based analysis to develop a holistic framework for evaluating post-impact damage severity. This framework quantifies reductions in structural capacity by considering uncertainties in material properties, geometry, and loading conditions. The aim is to support engineers in reaching informed decisions about serviceability and repair strategies for impacted piers without relying solely on traditional visual inspections or conservative assumptions.
- In pursuit of a non-destructive alternative to damage assessment, the study proposes a methodology that simulates extreme load events to estimate performance deterioration. This approach enables the evaluation of damage levels and failure risk without the need for full-scale destructive testing, offering a more efficient and cost-effective path toward ensuring structural safety and operational continuity.
- In short, the findings of this research contribute to a more nuanced understanding of RC pier performance under vehicular impact, particularly in the context of low-velocity collisions. By highlighting the influence of uncertainty in design parameters and post-impact conditions, the study lays the groundwork for improving both design practices and evaluation protocols. This ensures better preparedness for real-world impact scenarios, helping to enhance the resilience and longevity of bridge infrastructure.

Methodology

In this study, the performance of a prototypical traditional half-sized RC bridge pier is assessed under low-velocity vehicular impact loading through a combination of experimental testing and validated by numerical analysis using FEM. The investigation focuses on impacts from Class-I vehicles, specifically subcompact and mid-sized sedans, to evaluate the pier's residual capacity following such collisions and its ability to withstand subsequent events like earthquakes. Pendulum impact tests have been conducted to simulate vehicle crashes. These controlled low-speed impacts are intended to replicate cosmetic damage typical of real-world minor crashes. After impact, the specimens are closely delved to identify damage patterns and assess the reduction in structural capacity. The post-impact behavior has been analyzed to estimate the probability of failure (P_f) to determine the reliability index (β) under additional loading, offering insight into the resilience of RC bridge piers exposed to low-level vehicular collisions.

In the numerical investigation, the RC bridge pier model has been subjected to axial preloading to replicate in-service compressive forces and simulate equivalent nonlinear loading conditions induced by low-velocity vehicle impacts. The performance assessment focused on material properties, post-impact behavior, and cosmetic damage levels. FE simulations were conducted using the commercial software ANSYS, with input parameters derived from experimental testing, published literature, and manufacturer data.[9] Static numerical simulations have been performed to evaluate the short-duration post-impact response of the pier, including deformation patterns and failure mechanisms. These simulations are validated against experimental results for similarly configured RC piers under identical loading conditions, ensuring model accuracy and relevance.

The numerical model represented the RC pier as a composite structure, incorporating different materials modeled with non-separable contact definitions to closely capture real-world behavior under impact. For each crash scenario, detailed results were obtained, including deformation profiles, Von Mises stress and strain distributions, shear stress, maximum strain energy, and stress intensity. Beyond deterministic analysis, probabilistic methods are applied to account for uncertainties in material behavior and loading conditions.

The post-impact performance results obtained from FE simulations are utilized to assess the damage severity and determine the residual load-carrying capacity of the RC pier under subsequent cyclic loading. Reliability analyses are conducted for both the impact scenarios to estimate the P_f and corresponding β under low-velocity impact scenarios, supporting the validation of experimental findings and offering a robust framework for quantifying structural risk and residual performance under minor vehicular collisions.

Furthermore, the study offers a practical framework for evaluating whether traditionally designed RC bridge piers impacted by minor vehicular collisions can remain in service. By integrating experimental data with numerical simulations, the research captures the extent of damage and quantifies the performance of the impacted piers under sequential loading scenarios. The results demonstrate the feasibility of continuing service for such structures when the damage remains within cosmetic or non-critical limits. Overall, the findings present an effective tool for infrastructure managers and engineers to justify post-impact serviceability decisions, enhancing the safety and sustainability of aging bridge infrastructure.

Representative RC Pier

Material and geometric properties of RC pier

In this study, a circular RC pier section is selected as the representative model for analysis, with its geometric and material properties shown in Fig. 1. The pier is designed to emulate realistic bridge substructure conditions and has an unrestrained height of 8.4 feet (2.54 m), reflecting typical above-ground lengths used in practice. The cross-section of the pier is solid and circular, with an outer diameter (overall) of 20 in (0.51 m) and an inner diameter (core concrete) of 17 in (0.43 m). This hollow-core design helps reduce weight while maintaining sufficient strength and stiffness. The concrete used in the pier has a compressive strength of 7 ksi (48.26 MPa), a value commonly used for structural

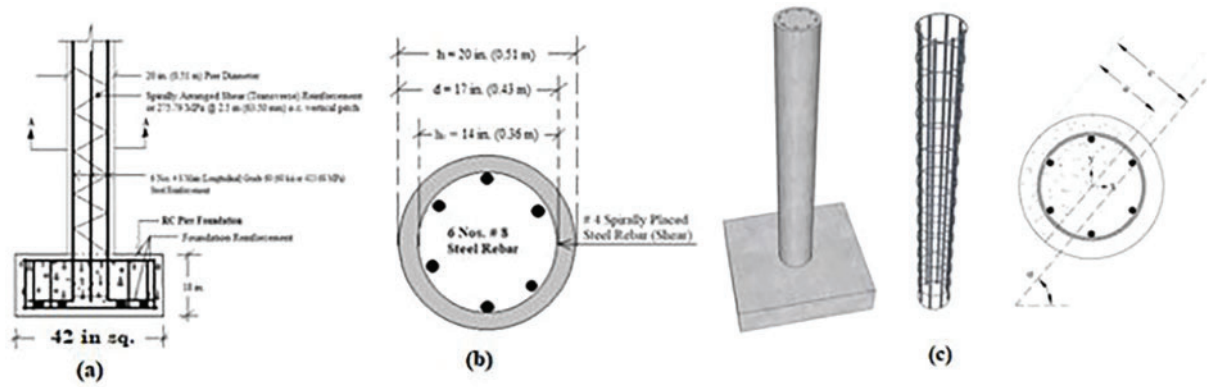

Figure 1. Reinforcement detailing of RC pier. (a) Sectional elevation, (b) Pier cross-section, and (c) 3D detailing. 3D, three dimensional

elements requiring high durability and load resistance. The reinforcing steel is specified as ASTM A706 Grade 60 with a yield strength of 60 ksi (413.68 MPa), selected for its superior ductility and weldability, which are crucial for seismic applications.

The pier's reinforcement configuration includes six longitudinal #8 bars placed symmetrically around the inner core to provide resistance against bending and axial loads. These bars extend fully into the foundation with a development length of 8 in (0.203 m), ensuring proper anchorage and load transfer. To resist shear forces and enhance ductility, #4 steel rebars with a yield strength of 40 ksi (275.79 MPa) are arranged in a spiral configuration at a center-to-center spacing (pitch) of 2.5 in (63.5 mm). This spiral arrangement conforms to the minimum shear reinforcement requirements outlined in ACI 318-11 and supports adequate confinement of the concrete core, which is essential for maintaining strength and energy dissipation capacity under cyclic and impact loading. Furthermore, the detailing complies with the recommendations by Furlong,[10] ensuring that both rebar diameter and spiral pitch meet established safety and performance criteria. This reinforcement layout enables the pier to develop sufficient ductile behavior and structural resilience under multiple loading conditions, including seismic and vehicular impacts.

The details of the representative RC pier are further shown in Table 1.

Table 1 summarizes the key geometric and material properties of the representative circular RC pier section used in this study. The symbol h denotes the outer diameter of the pier, while d represents the inner diameter as stated, defining the uniform circular section. The gross cross-sectional area of the pier is given as A_g, while A_{st} indicates the total area of the main (longitudinal) reinforcing steel bars embedded in the pier section. The net cross-sectional area, denoted by A_{net}, refers to the effective concrete area available for axial and flexural resistance.

The material strengths are represented by f_c' for the compressive strength of concrete and f_y for the yield strength of the reinforcing steel. Additionally, the reinforcement ratios are expressed as ρ_l and ρ_t, representing the longitudinal (main) and transverse (spiral) steel ratios, respectively. These parameters provide a comprehensive understanding of the pier's reinforcement layout and material capacity, serving as critical inputs for both the experimental evaluation and numerical simulations conducted in the study.

Experimental Program of Test Pier Specimens

In analyzing and determining the post-impact residual capacity of the RC pier in the test program, five prototype pier specimens with circular cross-sections were considered and tested. The specifications for the RC bridge pier were taken from a standardized state department of transportation detail.[11] The representative pier is modeled as having a uniform solid circular cross-section with a constant overall diameter of 20 in. (50.80 cm) throughout its length. The unrestrained length of the pier is 8 feet 4 in (2.54 m). A concrete cover of 1.5 in. (3.81 cm) is provided as per standard specifications. The boundary conditions for the pier are such that the bottom end is fixed, restraining displacement and rotation in all directions, while the top end is also fixed, preventing displacement and rotation, as shown in Figs. 3a and 3b. A schematic diagram illustrating these end conditions is provided in Fig. 3b.

For each representative RC pier, a square foundation has been designed in accordance with established design procedures to resist both static and dynamic impact loads. The foundation has a square plan measuring 3 ft 6 in. × 3 ft 6 in.

Table 1. Details of the representative pier

h (in.) (cm)	d (in.) (cm)	A_g (in.^{2}) (cm^2)	A_{st} (in.^{2}) (cm^2)	A_{net} (in.^{2}) (cm^2)	ρ_l (%)	ρ_t (%)	f'_c (ksi) (MPa)	f_y (ksi) (MPa)
20 (50.80)	17 (43.18)	314.28 (2027.60)	4.74 (30.58)	309.54 (1997.02)	1.5	0.06	7.00 (48.26)	60 (413.68)

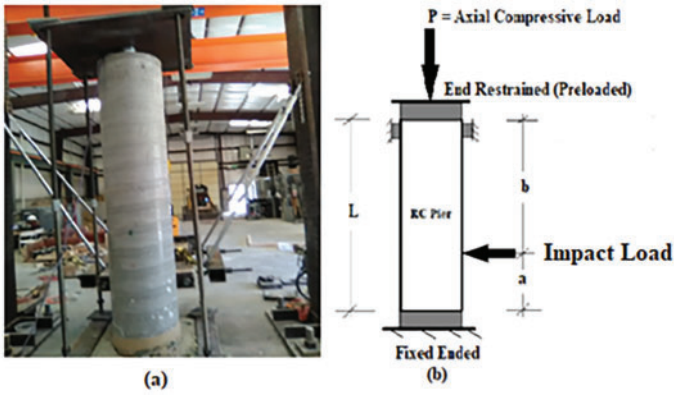

Figure 2. (a) Test specimen, and (b) schematic diagram of pier end conditions

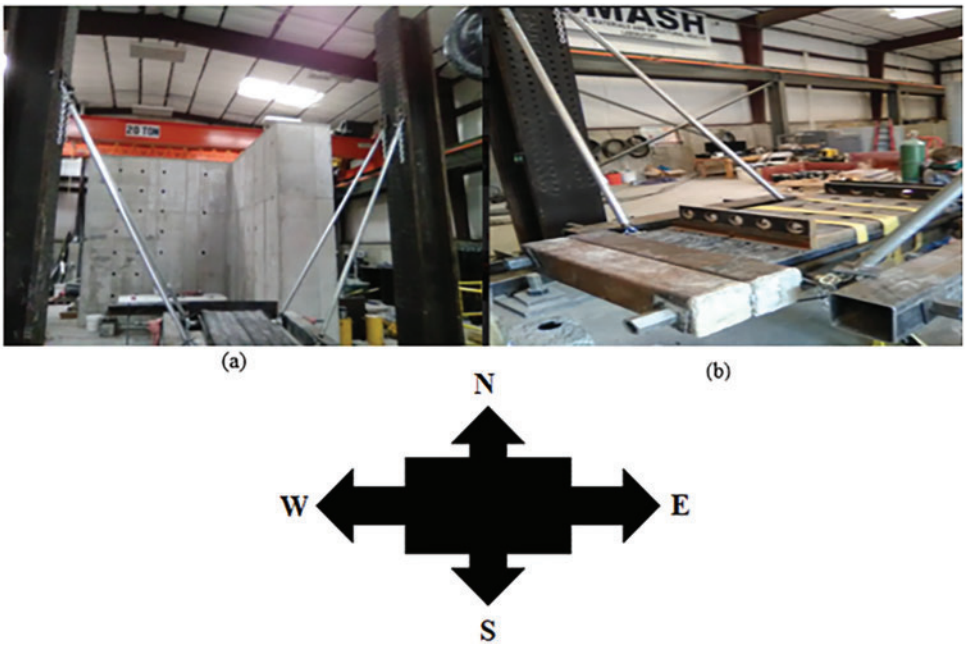

Figure 3. Pendulum impactor with weights. (a) 17.50 kips and (b) 22.50 kips

(106.68 cm × 106.68 cm) with a thickness of 1 ft 8 in. (53.34 cm), as shown in Fig. 1. Each foundation was fabricated to anchor the pier to the strong floor using 4 in (≈100 mm) diameter and 16 ft (≈4.87 m) long high-strength anchor bolts, thereby replicating a fixed-base boundary condition. At the opposite end, the pier was provided with a pinned boundary condition, as shown in Fig. 2, and axial preloading was imposed to simulate realistic support conditions.

To evaluate the serviceability and post-impact response of circular RC bridge piers subjected to vehicular collisions, representative prototype pier specimens (depicted in Figs. 2a and 2b) are analyzed. The pier's design specifications are based on experimental data obtained from tests conducted at the high-precision "Structural Laboratory" at Utah State University, Logan, Utah, USA. The pier is modeled with a uniform circular cross-section throughout its entire height to accurately reflect its structural behavior. Regarding the boundary conditions, the top end of the pier is modeled as a hinged (pinned) support. Translational displacement is permitted only in the direction of the applied impact force, while translational movements in all other directions are restrained. Rotational degrees of freedom are left unrestrained. The bottom end of the pier, representing the foundation interface, is fully fixed, preventing any displacement or rotation, as illustrated in Fig. 2.

Test setup for pendulum impact test

The pendulum system is supported by four arms and anchored to rigid steel columns, enabling free swing through a calibrated quick-release mechanism. The detailed configuration of the pendulum impact test setup is presented in Fig. 3.

Pendulum-based impact testing is widely employed to simulate vehicle–bridge pier collision scenarios and to investigate the associated dynamic response characteristics and damage mechanisms.[12] In the present study, the impact energy imparted to the pier resulted in deformations that have been observed to be negligible within the measurement limits.

A schematic representation of the pendulum system, including the direction of load application and the overall experimental arrangement, is shown in Fig. 3.

Determination of pendulum weights

In-built pendulums have been used in the experimental program to replicate the impact energy imparted to the pier by representative Class-I vehicles. Vehicle weights of 3.36 kips (14.95 kN) for a mid-sized sedan and 2.51 kips (11.14 kN) for a subcompact car are adopted based on the data reported by Thomas et al. (2018). Corresponding impact velocities of 22.87 mph (33.54 ft/s or 36.80 km/h) and 21.38 mph (32.83 ft/s or 36.02 km/h) were reproduced using the pendulum system, thereby simulating realistic vehicle–pier collision conditions.

The impact energy (E) imparted by these collisions is calculated from the kinetic energy (KE) using the standard equation shown in Eq. (1).[13] This calculation is essential to quantify the energy absorbed by the pier during impact, allowing for a precise assessment of its structural response under these controlled yet realistic conditions

$$E = 0.5 * M_{veh} * V_I^2 \tag{1}$$

where E is the total impact energy, M_{veh} designates the vehicle masses (Class-I), and V_I is the impacting velocity of the car.

As the total impacting energy does not get transformed into crash energy due to dissipation caused by column stiffness,[4] as well as the frontal stiffness and recoiling action of the impacting body.[4,14] To conduct the experimental methods and extracting results into real crash scenarios, the energy dissipation ratio (k) is considered as 0.72.[15] Thus, the effective energy ratio can be considered as (1 – k). The effective energy (E_{Eff}) can be estimated by using the Eq. (2).

$$E_{Eff} = (1 - k) \cdot E \tag{2}$$

where E_{Eff} is the effective energy causing damage to the column, k is the dissipation ratio, and E represents the energy incurred and transmitted from vehicle impact.

In order to reproduce a similar impact scenario, pendulum weights (W) used in the experiment can be computed from Eq. (3)

$$W = \frac{E_{Eff}}{g_{altitude} \cdot (h)} \tag{3}$$

where $g_{altitude}$ is the acceleration due to gravity (ft/s^2) considered as 32.16 ft/sec^2 (9.8 m/s^2) at a high altitude of 4,777 feet (1456.03 m), and h is the height of fall for pendulum, which is considered as 7 feet (2.438 m).

From the above Eqs. (1) through (3), weights of the pendulum are computed as 1.75 kips (7.78 kN) and 2.25 kips (10.01 kN), respectively, in order to reproduce the vehicle impacts caused by Class-I category of vehicles.

Test procedure

Pendulum impact experiments were conducted on a series of RC pier specimens, designated P1 and P2, using custom-fabricated pendulums with weights of 1.75 kips (7.78 kN) and 2.25 kips (10.00 kN). The pendulums were designed and assembled in such a manner that they can deliver controlled impact forces, as shown in Fig. 3. The pier specimens were subjected to impact loading generated by a pendulum released from a drop height of 7 ft (2.13 m). A schematic of the experimental setup, along with the step-by-step testing procedure, is presented in Fig. 4, providing an incisive representation of the test configuration and methodology.

Fig. 4 provides a schematic representation of the structural system and pendulum assembly. The test column of height H = 8.4 ft (2.56 m) supports a horizontal beam at elevation h = 7.0 ft (2.13 m). A pendulum of weight W is suspended from the beam, forming an angle θ with the vertical, as shown. The applied lateral load from the swung pendulum at the column base is denoted by P.

To determine the equivalent impacting vehicle velocities corresponding to lower vehicle weights, as presented in Table 3, two representative vehicle classes were selected to simulate low-impact collision conditions: a subcompact car (2.51 kips or 11.14 kN) and a mid-sized sedan (3.36 kips or 14.95 kN).[16] These vehicles were chosen due to their prevalence in urban traffic environments and their relatively lower weights, which reduce KE during collisions compared with heavier vehicle types. This selection allows for a more accurate assessment of short-duration impact energy transfer and structural response under low-to-moderate and cosmetic collision scenarios.

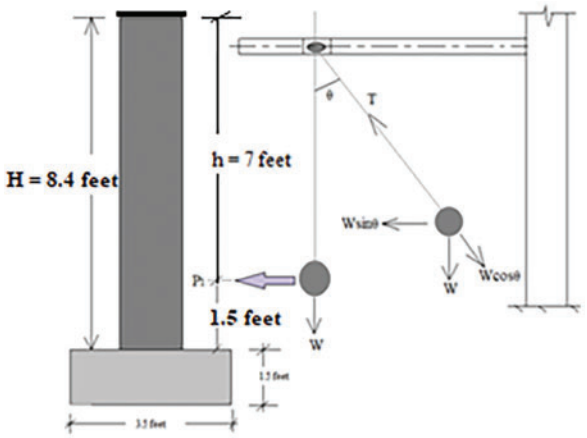

Figure 4. Schematic diagram for pendulum impact experiment

The impacting vehicle velocities (V_I) are estimated assuming approximately 72% energy dissipation, following the methodology proposed by Li et al.,[15] as expressed in Eq. (4).[17] This dissipation factor reflects the proportion of KE absorbed by vehicle deformation, frictional losses, and restitution during impact, providing a more realistic representation of actual crash dynamics. Incorporating this energy loss into the velocity computation ensures that the equivalent velocities derived more accurately capture the mechanical behavior of real-world collisions rather than idealized, perfectly elastic impacts

$$V_I = \sqrt{\frac{W..g_{altitude} \cdot h_I}{0.14 \cdot (M_{veh})}} \tag{4}$$

Rearranging Eq. (4), the final expression for determining the vehicle impacting speed is shown in Eq. (5).[17]

$$V_I = 2.67\sqrt{\left(\frac{W}{M_{veh}}\right) \cdot (g_{altitude}) \cdot (h_I)} \tag{5}$$

where W, M_{veh}, $g_{altitude}$, and h_I represent pendulum weight, weight of the impacting vehicle, acceleration due to gravity at specific altitude as already mentioned, and height of fall for impact. The impacting velocities are given in Table 2.

FEM

In this study, a detailed FEM of the RC test pier specimen was developed to simulate and analyze its behavior under low-velocity car crashes. The FEM was specifically designed to capture the nonlinear response of the pier during low-velocity car crash events, enabling accurate prediction of the post-impact structural performance and residual capacity. To validate and complement the experimental results, two pier models subjected to higher preload conditions, reflective of those applied during physical testing, were investigated. These preload levels are critical for simulating the in-service stresses and boundary constraints the piers experience prior to impact. The pier geometry employed in the simulations

Table 2. Equivalent car impacting velocities

Car type	Picture	Car weights in kips (kN)	Pendulum weights in kips (kN)	Height of fall in ft (m)	Car impacting velocities in ft/sec (m/s)	Car impacting velocities in mph (kmph)
Subcompact car		2.51 (11.14)	1.75 (7.78)	7 (2.13)	33.54 (10.22)	22.87 (40.46)
Mid-sized sedan car		3.36 (14.95)	2.25 (10.00)	7 (2.13)	32.83 (10.00)	22.38 (43.53)

replicates the physical specimens exactly, as shown in Fig. 5, ensuring consistency between experimental and numerical analyses.

The modeled piers were subjected to impacts from Class-I vehicle types, which correspond to commonly encountered vehicles in typical collision scenarios and are frequently used as standard references in impact testing. The detailed specifications of these vehicles, including weight, size, and impact velocity, are outlined in Table 3, ensuring that the simulation parameters closely mimic real-world conditions. By accurately representing these vehicle characteristics and their interaction with the pier, the numerical model provides a comprehensive insight into the pier's dynamic response, including stress distribution, damage initiation, and energy absorption mechanisms. This realistic simulation framework is crucial for evaluating the pier's post-impact durability and structural integrity, ultimately aiding in the design of safer and more resilient infrastructure capable of withstanding vehicle collisions.

Figure 5. FE model of test pier specimen

Loading conditions of the representative RC pier

Low-velocity car impact

Traditionally, bridge piers have been designed primarily to withstand static loads, such as axial forces, shear stresses, bending moments, bond stresses, and ensuring adequate development length for reinforcement. These static considerations have formed the basis for most design codes and practices due to their predictability and relative simplicity. However, in recent years, the importance of dynamic loading conditions has gained greater recognition, especially in the context of extreme events such as vehicle impacts, blasts, and earthquakes. Unlike static loads, dynamic loads introduce time-dependent forces that can cause rapid changes in stress and strain, leading to complex structural responses including vibrations, localized damage, and sometimes catastrophic failure modes up to complete collapse.

To effectively evaluate the effects of impact loads on RC piers, engineers often convert the dynamic impact forces into an equivalent static force. This simplification allows for practical design and analysis by approximating the maximum effects of dynamic loading through a static load case that represents the peak force during impact. Although this method does not capture the full time-history response of the structure, it provides a conservative and computationally efficient means to assess structural safety under impact scenarios. The specific loading conditions applied to the prototype RC bridge pier in this study are illustrated in Fig. 6, highlighting how the forces are assumed to act on the pier during impact. This representation aids in bridging the gap between complex dynamic behavior and practical engineering design, ensuring that the pier's resilience and performance under impact conditions can be reliably assessed and improved.

In this study, the equivalent car (Class-I) impact results are replicated. The impact duration considered for these analyses is 0.21 s, which is appropriate for the quasi-static impact and the corresponding results are utilized to determine low-velocity impacts using Eq. (6)

$$I_F = (M_{veh} * V_{veh})/t \tag{6}$$

where M_{veh} represents the weight of the impacting vehicle, V_{veh} is the frontal impact velocity of the vehicle causing

Table 3. Car crash data

Car type	M_{veh} (kips)	V (feet/sec)	T (sec)	I_F (kips)	Preload (kips)
Subcompact	2.505	33.54	0.207	405.88	50
Mid-sized sedan	3.361	32.83	0.207	533.05	75

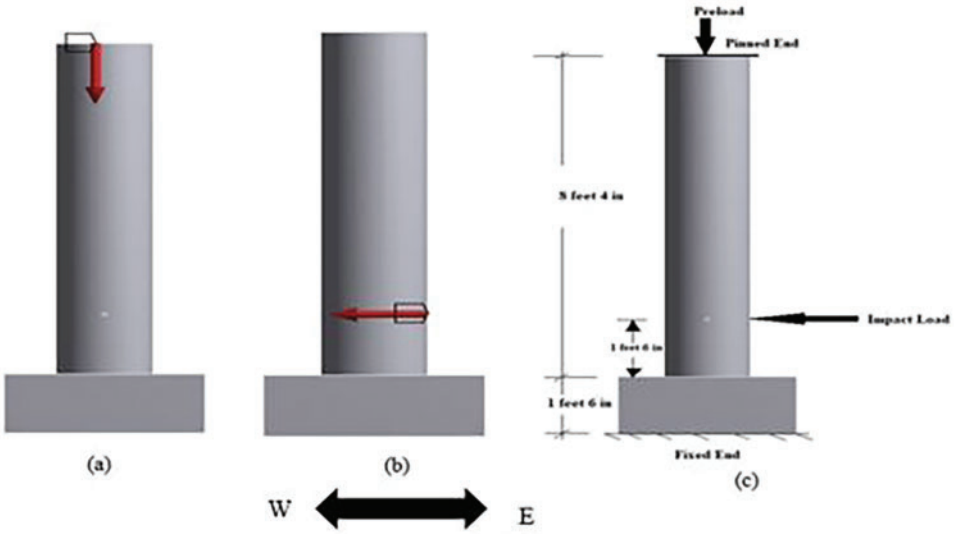

Figure 6. Pier for (a) preloading, (b) car impact loading, and (c) combined loading scenario

instability of the column, and t is the duration of impact. Impact duration for heavy to mid-sized cars may vary from a very short duration of 40 ms[14] to 0.21 s for quasi-static to dynamic strain rate loading (Roy et al., 2021). In this study, impact duration is considered as 0.21 s because of the quasi-static short-duration impact. However, the car crash data, as applied on the prototyped representative RC bridge pier along with the applied preloading, are shown in detail in Table 3.

Material properties

The FE analyses (FEA) have been carried out using models that precisely replicate the actual geometrical configurations, material properties, and boundary conditions of the tested RC piers. This high-fidelity modeling approach enables a realistic simulation of the piers' structural behavior under diverse loading scenarios, ensuring that the numerical outcomes are consistent with experimental observations. By carefully defining each geometric and material parameter, the FE models can accurately capture stress distributions, deformation patterns, and local failure modes, thereby enhancing the reliability of the analytical outcomes.

Table 4 summarizes the key input parameters, including the compressive strength of concrete, mechanical properties of the reinforcing steel, and other critical material characteristics that govern the nonlinear response of the structure. These parameters play a vital role in simulating complex behaviors such as cracking, yielding, and energy dissipation during impact loading. Incorporating these detailed material definitions allows the FE model to reproduce the progression of damage and the post-impact residual capacity of the piers, providing valuable insights into their performance and resilience under extreme loading conditions.

For all material interfaces within the FEM, a non-separable contact condition is applied to accurately represent the interaction between different components, such as concrete and reinforcing steel. This ensures that the elements remain bonded during the analysis and that no relative motion occurs at the interfaces, which is critical for simulating realistic stress transfer and failure mechanisms. In terms of boundary conditions, the external peripheral surface of the column is considered free, allowing natural deformation, while the top face of the column is modeled as pinned, restraining translational movement but allowing rotation. The foundation base is modeled as fully fixed, preventing any displacement or rotation to replicate the actual test setup and anchorage conditions.

A detailed three-dimensional (3D) FE model of the RC pier has been developed, incorporating accurate geometry, material properties, and boundary conditions. Non-separable contacts ensured proper interaction between materials, while the top of the pier was modeled as pinned and the foundation as fixed. This model, shown in Fig. 7, served as the basis for simulating the structural response under impact loading.

Mesh and boundary conditions for FE model

A comprehensive mesh-independence study has been performed to determine the optimal mesh size for the FE

Table 4. Material properties

Materials	Material properties and respective values	
Concrete	Modulus of elasticity (psi) (MPa)	$3.6 * 10^6$ ($2.48 * 10^4$)
	Poisson's ratio	0.18
	Open shear transfer coefficient	0.3
	Closed shear transfer coefficient	1
Reinforcing steel (main)	Modulus of elasticity (psi) (MPa)	$2.9 * 10^7$ ($1.9 * 10^5$)
	Poisson's ratio	0.3
	Yield stress (psi) (MPa)	60000 (413.68)
	Tangent modulus (psi) (MPa)	2900 (19.995)
Reinforcing steel (transverse)	Modulus of elasticity (psi) (MPa)	$2.9 * 10^7$ ($1.9 * 10^5$)
	Poisson's ratio	0.3
	Yield stress (psi) (MPa)	40000 (275.79)
	Tangent modulus (psi) (MPa)	2900 (19.995)

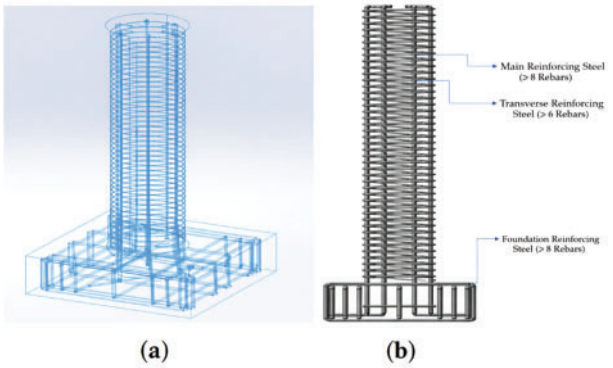

Figure 7. (a) Three-dimensional (3D) reinforcement using solid works and (b) 2D reinforcement detailing

simulations, ensuring a balance between computational efficiency and numerical accuracy. Through multiple refinement trials, the mesh was optimized to capture localized stress concentrations and potential failure regions without excessive computational cost. Non-separable contact definitions were implemented for all materials listed in Table 4, allowing for realistic interaction and load transfer between the concrete, longitudinal, and spiral reinforcements. A smooth transition between mesh densities was achieved using a transition ratio of 0.272, resulting in a total of 1,345,129 elements and 3,736,988 nodes, parameters that collectively guarantee stable convergence and physically consistent results.

The selected mesh sizes of 4.0 in. (101.60 mm) for concrete, 0.25 in. (6.35 mm) for longitudinal reinforcement, and 0.125 in. (3.175 mm) for spiral reinforcement have been chosen based on the structural significance of each component and their associated yield strengths of 60 ksi (413.68 MPa) and 40 ksi (275.79 MPa), respectively. The boundary conditions are configured to simulate the experimental setup accurately, with the pier's top fixed against displacement and rotation, while the foundation base has been fully restrained in all directions, as illustrated in Fig. 5. The meshing configuration shown in Fig. 8 demonstrates the fine discretization

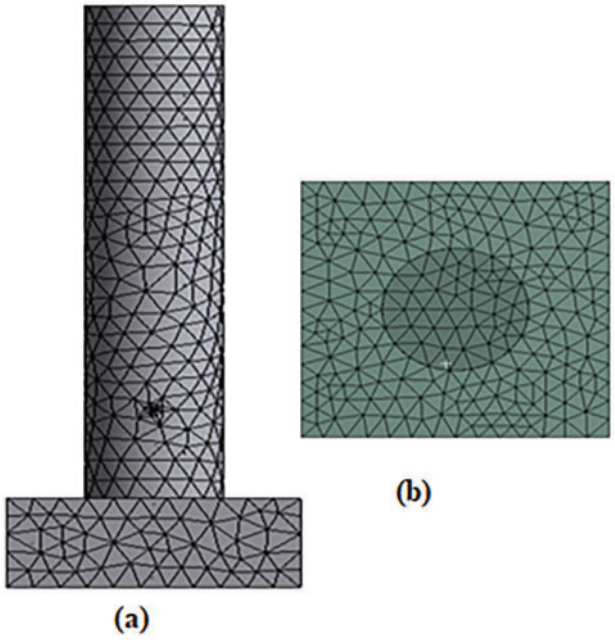

Figure 8. Meshing of FEM for (a) Combined mesh model with impacting point and (b) plan of concrete element

in critical regions and the smooth transitions that minimize numerical artifacts, ensuring reliable simulation of stress propagation and deformation behavior under applied loads.

Impact Damage Assessment Using Reliability Analyses

In this research, a probabilistic framework is adopted to evaluate the structural performance of RC piers subjected to low-velocity car crashes as already discussed. Specifically, reliability analysis is employed to quantify the likelihood of structural failure and assess the extent of damage. The analysis follows the resistance–load approach, wherein

uncertainties in both structural capacity (resistance) and external demands (impact loads) are considered. To evaluate post-impact performance, the resistance reduction method (RRM) is used, which involves reducing the pier's resistance incrementally and computing the corresponding probability of failure (P_f). This method enables a detailed understanding of how impact-induced damage affects the residual strength of the pier. The test pier is thus assessed not only in terms of whether it fails under impact but also to evaluate its reduced load-carrying capacity diminishes, providing a comprehensive insight into its post-collision structural reliability.

Pier resistance

Prior to computing the residual capacities, the design capacities in axial and shear for the representative RC pier are computed as specified in ACI.[18]

The design axial capacity ($P_{N,design}$) is computed as shown in Eq. (7)[19]

$$P_{N,design} = 0.85 * f_c' * \left(A_g - A_s\right) + \sigma_y * A_s \tag{7}$$

where f_c' is the 28-day compressive strength of concrete, f_y is the yield strength of steel, and A_g and A_{st} are the gross cross-sectional area of concrete and total cross-sectional area of longitudinal steel, respectively. $P_{N,design}$ is computed as 2126.16 kips (11,034.61 kN) and shown in Table 5. The axial load (preloading) applied on each test specimen was initially considered as 80% of the axial capacity and are as shown in the Table 3. The detailed considered preloading estimated from design strength is as shown in Table 5.

The design shear capacity of the RC bridge pier is determined using Eq. (8)[20]

$$V_{N,design} = V_c + V_s \tag{8}$$

where V_c is the shear strength carried by the concrete and V_s is the transverse shear capacity.

The shear strength, V_c, is computed as shown in Eq. (9)[21]

$$V_c = \nu_b[1 + 3P_{N,design}/f_c' \cdot A_g] \cdot A_e \tag{9}$$

where A_g represents the gross cross-sectional area of the concrete in the pier and A_e is 80% of A_g, i.e., $A_e = 0.8 * A_g$, and ν_b is the shear constant.

The shear constant (ν_b) is determined using Eq. (10)[21]

$$\nu_b = [0.0096 + 1.45\rho_t] \cdot \left(f_c'\right)^{1/2} \leq 0.03\left(f_c'\right)^{1/2} ksi \tag{10}$$

where ρ_t is the longitudinal steel ratio and $P_{N,design}$ represents the axial load capacity of the RC pier.

The transversal shear capacity, V_s, is computed using Eq. (11)[21]

$$V_s = (\pi/2)(A_h\sigma_{yh}) \cdot (D'/s) \tag{11}$$

where A_h is the area of a single hoop or spiral, D' is the spiral or hoop diameter, s denotes the pitch of the helix, and σ_{yh} represents the yield stress of transverse reinforcing steel.

Load

The equivalent Class-I vehicle impact responses have been replicated from the pendulum impact experiments to establish representative loading conditions. The resulting impact parameters are subsequently incorporated into Eqs. (1)–(4) to evaluate the corresponding low-velocity impact effects. The computed results derived from this procedure are presented in Table 6.

Determination of post-impact damage

In this study, post-impact cosmetic damage to the RC pier is evaluated through a reliability-based assessment by determining the probability of failure under specific low-velocity impact scenarios. In the first stage, the reduction in structural resistance resulting from vehicle impact is estimated using the RRM, implemented through Monte Carlo (MC) simulations. This method allows for the incorporation of variability in material properties, loading conditions, and damage extent. Given the inherent uncertainty in quantifying residual capacity following low-impact events, deterministic analysis alone may not reliably capture the true probability of failure. Therefore, a probabilistic approach is employed to provide a more robust estimate of the

Table 5. Estimated preloading

$P_{N,design}$ (kips) (kN)	Preloading (kips) (kN)	Percent preload (Initial)
2126.16 (9457.63)	1063.08 (4728.81)	50

Table 6. Equivalent car impacting velocities[22]

Car type	Picture	M_{veh} in kips (kN)	V in feet/sec (km/hr)
Subcompact car		2.51 (11.14)	33.54 (36.80)
Mid-sized sedan car		3.36 (14.95)	32.83 (36.02)

post-impact performance, focusing particularly on cosmetic damage levels that may not lead to structural failure but still affect serviceability and safety perception.

LSE analysis method

Using Eqs. (11) through (14) and Eq. (16), it is evident that the load model is governed by the dynamic impact force, while the resistance model is characterized by the dynamic shear capacity of the pier. Both models incorporate parameters treated as random variables to reflect the inherent uncertainties in material properties, loading conditions, and structural response. A random variable is typically defined by its mean, standard deviation, and probability distribution, statistical descriptors that capture the variability and unpredictability associated with real-world conditions. Therefore, replacing nominal design values with their corresponding means and standard deviations allows for a more realistic representation of uncertainty in the probabilistic framework. This approach ensures that the reliability analysis captures the true variability in both loading and resistance, as recommended in Roy.[9]

However, structural serviceability for the limit state function (G_i) comprises the performance not exceeding the permissible function as shown in the Eq. (12). This shows the limit state equation (LSE) satisfying the serviceability criteria.[9]

$$G_I = 1 - \lambda = 1 - \frac{I_{dyn}}{V_{dyn}} \tag{12}$$

where G_I is the limit state function, I_{dyn} is the peak vehicle dynamic impacted force, and V_{dyn} indicates the dynamic shear effect on concrete as mentioned in the Section 3.3.

Nominally, the probability of failure (P_f) is determined by integrating the limit state function over the region where the limit state function is less than or equal to zero, as expressed in Eq. (13)[23]

$$P_f = \int_{Z=-\infty}^{Z\leq 0} f_x\,(x_1, x_2, \ldots, x_n)\,dx_1 dx_2 dx_3 \ldots\ldots\ldots dx_n \tag{13}$$

where f_x is the joint PDF of the random vector $\boldsymbol{X} = \{x_1, x_2, \ldots, x_n\}$, *and* $Z = g(x) < 0$; that is the region of failure. This is further illustrated within the region, $-\infty = Z \leq 0$, where the failure of the RC bridge pier due to vehicle impact is expected to occur.

Determining P_f by directly evaluating the integral in Eq. (16) is analytically complex due to the nonlinear nature of the limit state function and the presence of multiple random variables. As an alternative, structural reliability can be assessed using the β, which provides a simplified yet effective measure of safety. Unlike the probability of failure, which quantifies the likelihood of failure directly, the reliability index serves as a standardized metric that reflects the margin of safety while accounting for the inherent uncertainties in model parameters.[24] Various reliability methods have been developed to compute P_f and, consequently, estimate the corresponding β. However, β can also be determined from different simulations.

In this study, MC simulations are used to evaluate the P_f under low-velocity impact conditions, particularly focusing on cosmetic damage levels that may not result in structural collapse but still impact serviceability. While different reliability methods may yield slight variations in β and P_f, they offer consistent insight into the overall structural performance. In its most basic form, the reliability index is calculated using the mean and standard deviation of the load and resistance variables, as outlined in Eq. (14)[25]

$$\beta = \frac{\mu}{SD} \tag{14}$$

where μ is the mean of the LSE and SD is the standard deviation of the limit state equation.

However, computing μ and SD of the LSE is often impractical especially when the limit state is a nonlinear function. Also, it presents problems in dealing with limit state equations where the probability distribution is not normal. As a result, an alternate method of computing the β involves using MC simulations. This method involves simulating the LSE a number of times with changing design variables. These design variables are developed using the uncertainty parameters and randomly generated numbers as shown in Eqs. (15) and (16)[25]

$$x_i = \mu_x + z_i \sigma_x \tag{15}$$

$$z_i = \Phi^{-1}(u_i) \tag{16}$$

where x_i is the computed variable, z_i is standard normal variable, u_i are uniformly distributed random variables between 0 and 1, and Φ^{-1} is the inverse of the standard normal cumulative distribution function (CDF).

The LSE defines the boundary between safe and failure conditions for the structure, where a value less than zero indicates failure. To assess the P_f, this equation is iterated multiple times using randomly generated input variables, which represent the inherent uncertainties in material properties, loading, and geometry. These variables are typically sampled from uniform or other relevant probability distributions to cover a broad spectrum of realistic scenarios. By running thousands, or even millions of such simulations, the analysis captures the variability and randomness present in real-world conditions.

The P_f is then estimated as the ratio of the number of simulations in which the LSE yields a negative value (indicating failure) to the total number of simulations performed. This MC-based approach provides a statistically robust measure of risk without relying on overly simplistic assumptions. Once the probability of failure is obtained, the β can be estimated using established mathematical relationships (as shown in Eqs. (17) and (18)). The β essentially translates the P_f into a standardized safety metric, reflecting the number of SDs the system's performance is from the failure threshold. This allows engineers to quantify safety margins and make informed decisions regarding design and maintenance

$$P_f = \frac{n}{N} \tag{17}$$

$$\beta = -\Phi^{-1}\left(P_f\right) \tag{18}$$

where n is the number of times the limit state was exceeded ($g(x) < 0$), and N is the total number of simulations undertaken.

A recently developed method that addresses some of the challenges associated with traditional fault tree analysis is the RRM.[17] Fault tree analysis often struggles with capturing the nuanced degradation of structural capacity following impact events, especially at low velocities where damage may be subtle yet significant. The RRM overcomes this by focusing directly on the residual capacity of the structural member after the loading event. It does so by quantifying the P_f that arises due to impact-induced damage, thereby providing a probabilistic measure of how the structure's ability to carry loads has diminished.

Using this probabilistic framework, the method computes a resistance reduction factor, denoted as ζ_P, which is defined as the complement of the P_f. This factor serves as a scaling coefficient applied to the original, undamaged structural capacity, effectively adjusting it to reflect the reduced capacity after impact. The calculation of ζ_P is shown in Eq. (19) (Roy[9]; ASCE).[4,5] By integrating uncertainty and variability in damage assessment, the RRM provides a more realistic and reliable means of updating structural capacity post-impact, enhancing both safety evaluations and maintenance decision-making

$$\zeta_P = 1 - P_f \tag{19}$$

where ζ_P is the resistance reduction factor and P_f has already been explained.

Reliability analysis requires that design parameters be treated as random variables characterized by their statistical properties μ and SD, and probability distributions, which are essential inputs for calculating the β. Table 4 summarizes the random variables considered in this study along with their associated probability distributions. The geometric dimensions and material properties used as parameters are sourced from established literature,[25] ensuring that the analysis is grounded in validated data. Vehicle mass parameters are derived from weigh-in-motion data collected in Utah,[26] while vehicle speed parameters are taken from Hwang and Nowak's study,[27] reflecting realistic loading conditions. Notably, the pitch of the transverse reinforcement is assumed constant and thus excluded as a random variable in this analysis. A comprehensive list of design variables and their uncertainty parameters is presented in Table 7, providing a detailed overview of the factors influencing the reliability assessment.

Similar to the damage index (λ), the ζ_P provides a practical means to adjust the original design capacity of the pier to reflect its residual strength after impact damage. By multiplying the design capacity by this factor, the method explicitly accounts for the degradation caused by the collision, effectively reflecting the reduced capacity to a level that represents the pier's post-impact performance. This probabilistically derived reduced capacity offers a more realistic assessment of the structure's remaining load-carrying ability. The calculation for the reduced capacity using this approach is expressed in Eq. (20)

$$L_{Reduced} = \zeta_P * L_{Design} \tag{20}$$

where ζ_P is the resistance reduction factor evaluated via a probabilistic approach, L_{Design} is the design capacity, and $L_{Reduced}$ is the reduced capacity of the impacted pier at specific loading event.

The evaluation of $L_{Reduced}$ is essential for understanding the pier's residual strength and for assessing structural safety after extreme events. It enables engineers to identify critical damage thresholds, evaluate the need for repair or replacement, and improve design strategies for impact-resistant structures. In numerical and experimental analyses, this parameter serves as a key performance indicator that bridges observed damage patterns with quantitative measures of strength degradation, supporting data-driven decision-making in structural resilience assessment.

In this study, a total of ten thousand (10,000) MC simulations have been performed on the limit state function to evaluate the reduced structural capacity corresponding to a target P_f. The simulations are carried out by repeatedly sampling the input variables and evaluating the limit state function for each realization. The selected number of simulations was sufficient to ensure statistical convergence of the results, as confirmed by the stabilization of the estimated mean and standard deviation of the response parameters.

Random numbers required for the MC simulations have been generated using the *RAND* function in Microsoft Excel,[28] enabling the stochastic representation of uncertainties associated with material properties, loading conditions, and geometric parameters. The design variables considered in the analysis, along with their corresponding statistical properties and probability distributions, are summarized in Table 4.

Results

Experimental

This section presents results primarily focused on detecting cosmetic damage and structural collapse through push-over experiments. Observations of damage include the development of localized cracks, spalling, and concrete delamination, which serve as key indicators of the pier's post-impact condition.

The observed results document the progression and severity of damage sustained by the test specimens during impact, specifically highlighting localized cracks, spalling of the concrete surface, and internal delamination. These damage modes are critical indicators of structural distress and energy dissipation mechanisms under dynamic impact loading as shown in Fig. 9. Impact damages combined with preloading conditions are detailed in Table 8. A detailed summary of these observations is encapsulated in Table 8, offering a comparative view of the extent and type of damage across different specimens and impact scenarios.

FEM

Comprehensive structural analyses were performed on the representative RC pier to assess its post-impact performance under low-velocity collision conditions. Damage quantification was achieved by evaluating key numerical indicators such as deformation, equivalent static strain and stress

Table 7. Design variables and their uncertainty parameters

No.	Variables	Distribution	Mean	CoV	St. Dev.	Units
1	Diameter of pier (h)	Normal	20.00 (0.51)	–	0.25 (0.006)	in. (m)
2	Height of pier (L)	Normal	100.06 (2.54)	–	0.25 (0.006)	in. (m)
3	Vehicle weight (M_{veh})	Normal	Varying	0.235	–	kip (kN)
4	Vehicle velocity (V)	Lognormal	Varying	0.165	–	ft/s (m/s)
5	Core concrete diameter (d_c)	Normal	17.00 (0.43)		0.25 (0.006)	inches (m)
6	Yield strength of transverse Reinforcement (σ_{yt})	Lognormal	40770 (280.62)	0.116	4729.32 (32.55)	psi (MPa)
7	Compressive strength of concrete (f'_c)	Normal	Varying	0.18	–	psi (MPa)
8	Diameter of longitudinal reinforcement (d_l)	Normal	0.855 (0.021)	–	0.365 (0.009)	in. (m)
9	Yield strength of longitudinal reinforcement (σ_y)	Lognormal	67500 (465.40)	0.098	6615 (45.61)	psi (MPa)
10	Diameter of transverse reinforcement (d_t)	Normal	0.56 (0.014)	–	0.365 (0.009)	in. (m)
11	Confined hoop diameter	Normal	17.355(0.44)	–	0.365(0.009)	inches (m)
12	Stiffness (k)	Normal	1713045 (300.00)	0.2	342609 (60.00)	kip/in. (kN/m)
13	Pitch (s)	Deterministic	2.5 (0.06)	–	–	in. (m)

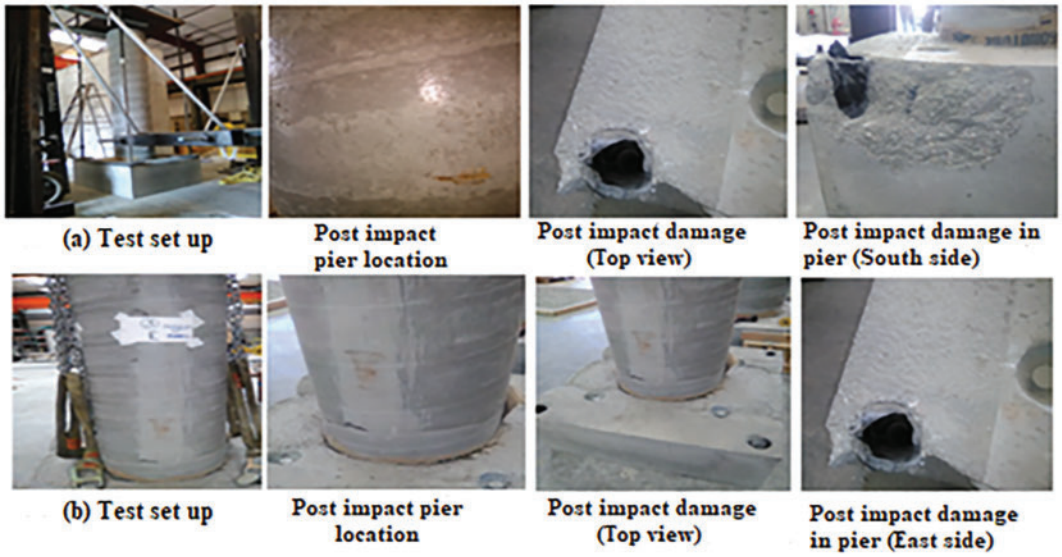

Figure 9. Pre-impact test setup and post-impacted pier damage for (a) P1 and (b) P2

(both based on the Von Mises criterion), shear stress, maximum strain energy, and stress intensity. These results are systematically presented in Figs. 10 and 11. Furthermore, high-resolution directional strain data were captured to provide a nuanced understanding of strain distribution patterns throughout the pier, with detailed visualizations shown in Figs. 12 and 13.

FE results of model for impacting subcompact car

The crash behavior of the representative RC pier specimen was simulated using a detailed FEM developed to capture the pier's response under impact loading. The FEM incorporated appropriate material models for concrete and reinforcement, realistic geometric details, and boundary conditions consistent with the experimental setup. The analysis captured the evolution of deformation and stress distribution throughout the pier during the impact event. The key results are presented in Fig. 10, which illustrates the deformation patterns and stress concentrations observed in the simulation. The simulation results show good agreement with the experimental observations, including the overall deflection shape and locations of maximum stress, indicating

Table 8. Results of pendulum impact testing

Column specimens	Preloading (kips)	Pendulum weights (kips)	Damage assessment			
			Damage location		Observations	Damage type
			Element type	Side		
P1	52	1.75	Foundation	South	Foundation damage	Spalling cracks along with delamination and edge cracking at the foundation concrete
P2	75	2.25	Foundation	East	Foundation damage	Spalling cracks along with delamination and edge cracking at the foundation concrete

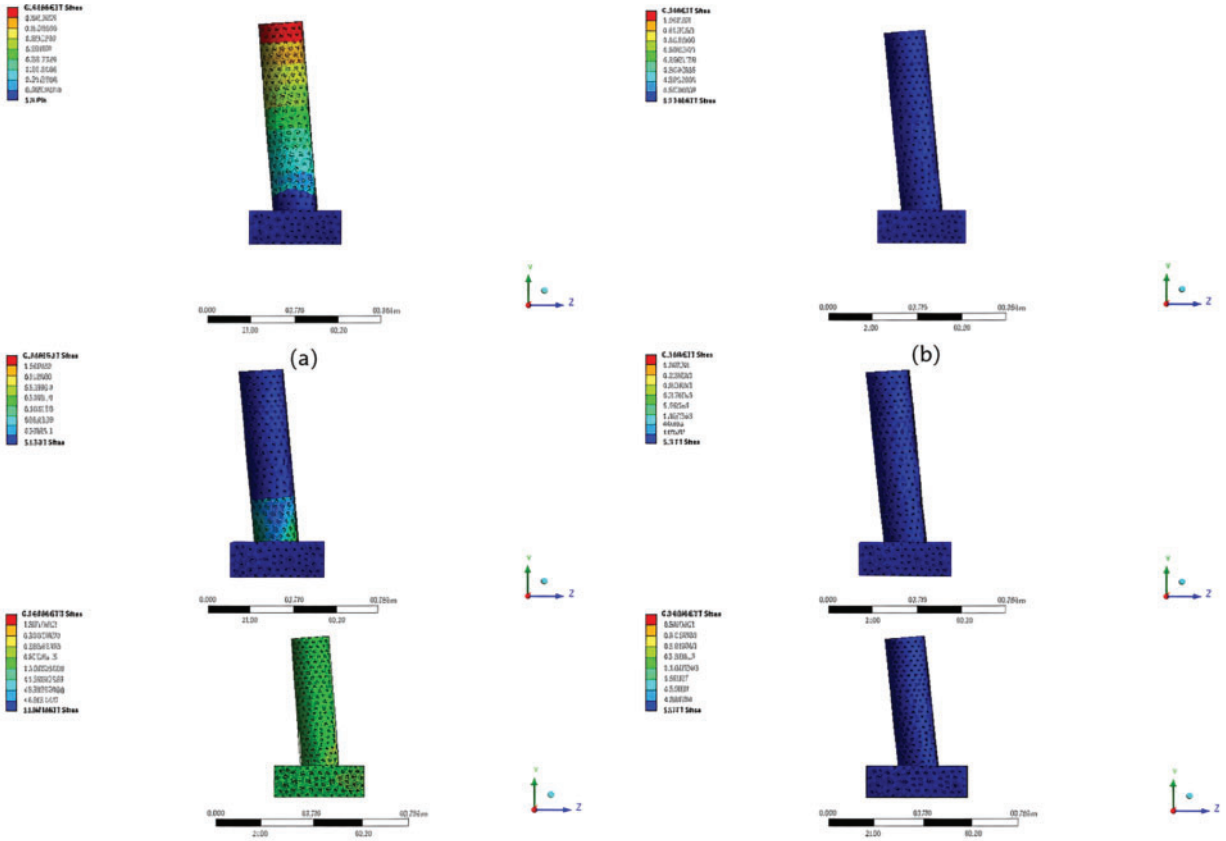

Figure 10. Subcompact impact results for (a) deformation, (b) Von Mises strain, (c) Von Mises stress, (d) Maximum Shear stress, (e) Maximum strain energy, and (f) Stress intensity

that the model provides a reliable representation of the pier's crash behavior.

FE results of model for impacting mid-sized sedan car

The impact response of the representative RC pier was simulated using a detailed FEM, with the results presented in Fig. 11. The simulation captures the dynamic interaction between the impacting body and the pier, revealing stress concentrations, crack initiation, and progressive damage throughout the structure. These results provide insight into the pier's deformation patterns, energy absorption capacity, and overall structural performance under impact loading. By highlighting the regions of maximum stress and localized failure, the FE analysis not only validates the accuracy of the

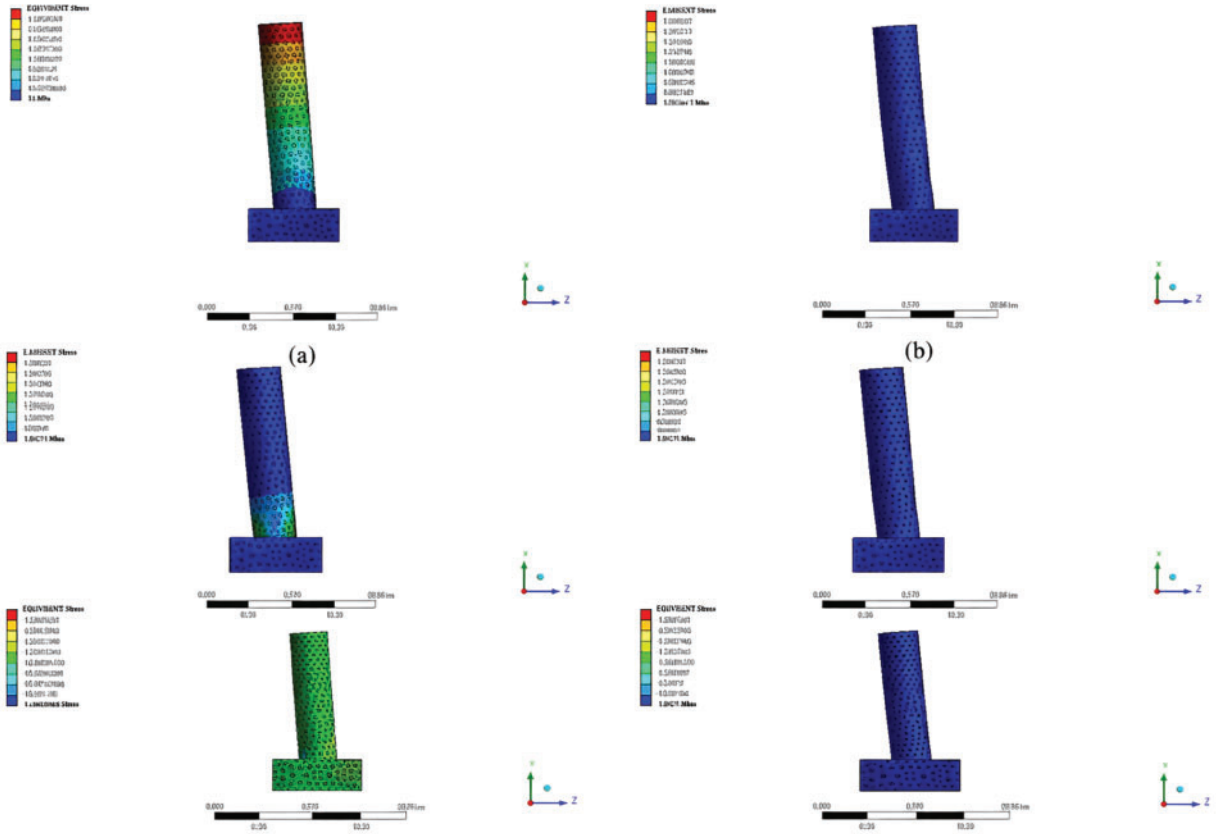

Figure 11. Subcompact impact results for (a) deformation, (b) Von Mises strain, (c) Von Mises stress, (d) maximum shear stress, (e) maximum strain energy, and (f) stress intensity

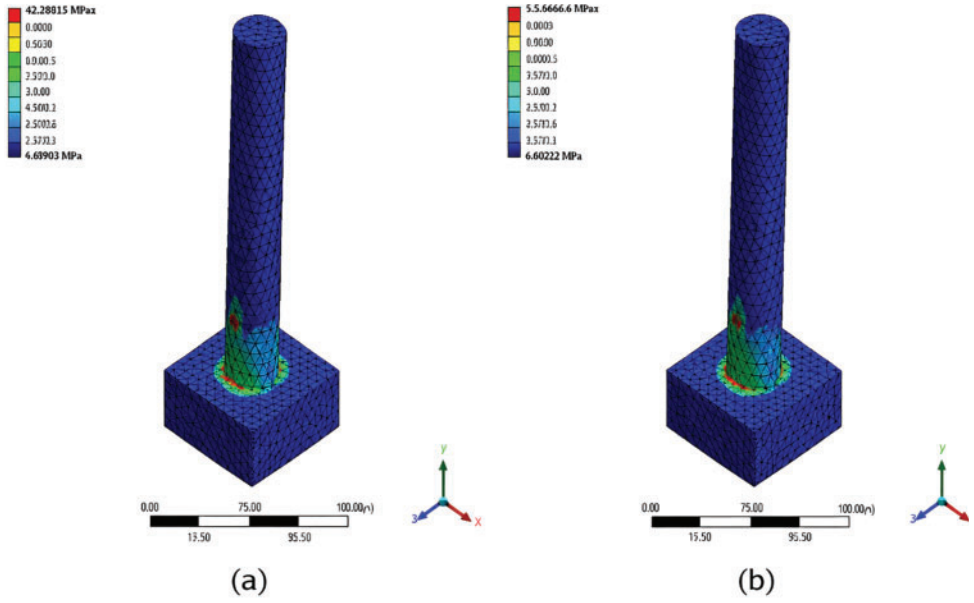

Figure 12. Three-dimensional view of high-precision stress concentration results due to impact from (a) Subcompact car and (b) Mid-sized sedan car

modeling approach but also offers a quantitative basis for assessing residual strength, performance degradation, and the effectiveness of design parameters in mitigating impact-induced damage.

Maximum stress concentrations and deformations were observed at the junction between the pier base and the foundation, as illustrated in Figs. 11 and 12. To better understand the failure mechanisms, high-precision stress concentration

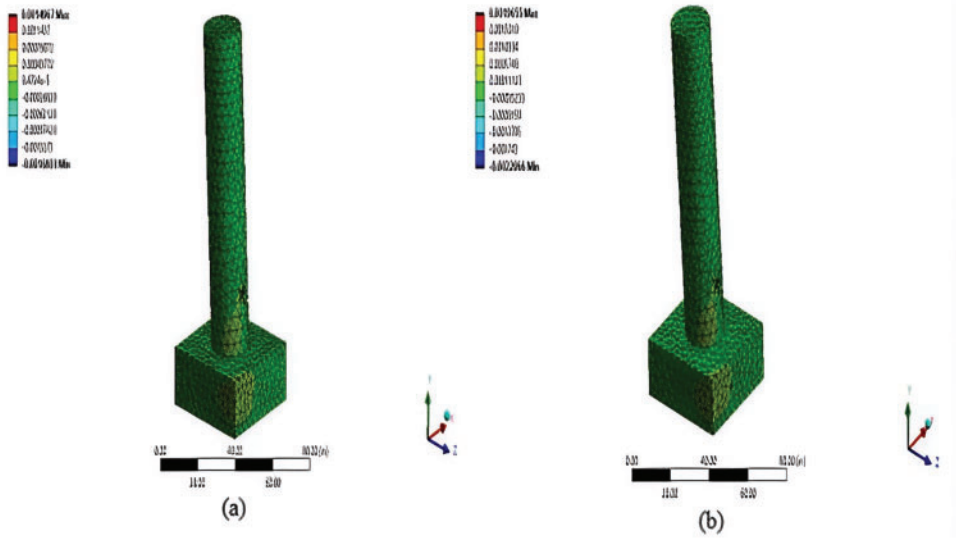

Figure 13. Three-dimensional view of high-precision directional deformation results due to impact from (a) subcompact car and (b) mid-sized sedan car

Table 9. Results from FEM

Pier specimens	Preloading (kips)	Pendulum weights (kips)	Damage assessment			
			Damage location		Observations	Damage type
			Element type	Position		
P1	52	1.75	Foundation and pier–foundation	Foundation edge and corners	Pier and foundation are highly stressed and deformed	Highly stressed zones are pier–foundation junction and foundation edge
P2	75	2.25	Foundation and pier–foundation	Foundation edge and corners	Pier and foundation are highly stressed and deformed	Highly stressed zones are pier–foundation junction and foundation edge

data were rescaled and compared in Fig. 12, which highlights the critical damage patterns in this region. The results indicate that the pier–foundation interface is the most vulnerable location under vehicle impact loading, where stress accumulation and structural deformation are most pronounced.

Variations in the simulation results reflect the inherent complexities involved in accurately modeling material behavior under post-impact conditions resulting from vehicle collisions. Despite these uncertainties, the analysis clearly shows that increasing impact loads significantly intensify the extent of structural damage. This trend is further supported by the directional deformation results presented in Fig. 13, where higher impact forces correspond to larger deformation magnitudes, confirming the direct relationship between impact intensity and structural response.

Results captured and extracted from FEA, summarized in Table 9, offer valuable insights into the structural response of the RC pier under impact loading. The simulations reveal pronounced stress concentrations, particularly at the pier–foundation interface and along the periphery of the foundation. Potential load transmittance paths followed by stress concentration-induced cracks are observed. These zones of elevated stress are critical, as they mark potential sites for the initiation and propagation of complex damage mechanisms such as cracking, spalling, or even localized structural failure.

The identification of these stress hotspots highlights inherent weaknesses in the structural system, emphasizing the need for careful design attention and potential reinforcement at these critical junctions. By pinpointing the most vulnerable areas, the FEM analysis not only aids in anticipating failure modes but also supports the development of targeted retrofitting and strengthening strategies to improve impact resilience. Overall, these findings demonstrate the indispensable role of detailed numerical modeling in capturing complex stress distributions, insights that are often missed by conventional or simplified design approaches.

Model validation

The developed FEM demonstrates a strong compatibility in predicting the post-impact behavior of the test pier, closely mirroring the physical damage observed during experimental testing. In particular, the model successfully captures critical failure modes, such as corner cracking and localized deformation, by analyzing directional displacement patterns. This precise replication of failure mechanisms not only confirms the model's accuracy but also provides valuable insight into stress concentrations and material responses at vulnerable locations. The consistency between the simulated deformation and the experimentally observed crack propagation, as illustrated in Fig. 14, validates the FE model as a reliable tool for assessing structural performance under impact loading, thereby supporting its use in design evaluation and damage mitigation strategies.

Although the car crash occurred at a relatively low velocity, Fig. 14 reveals that significant cracking developed at the foundation corners, warranting load transmittance path. These cracks propagate vertically along the anticipated load transfer paths, suggesting that even under modest impact energy, localized stress concentrations can be sufficient to initiate damage. This phenomenon indicates that the corners of the foundation act as critical stress increment locations where structural discontinuities or geometric features lead to an intensification of stress. The vertical crack propagation aligns with the direction of force transmission, implying a brittle or quasi-brittle failure mode typical of materials like concrete under tension.

The FE simulations, shown in Fig. 14, model pendulum impacts of 1.75 and 2.25 kips to represent the sequential increase in loading conditions. These simulations effectively replicate the experimentally observed patterns of crack initiation and growth, demonstrating the model's sensitivity to incremental damage development. The FE model captures both the spatial location and directionality of the cracks, indicating a high fidelity in stress distribution and fracture prediction. This strong correlation between simulated and experimental results not only validates the accuracy of the FE model but also reinforces its capability to simulate progressive damage mechanisms under repeated or escalating impact loads, a critical consideration for evaluating structural resilience in real-world crash scenarios.

Reliability analyses

A rigorously undertaken MC simulation involving 10,000 iterations has been performed on the LS function (g_i), with statistical parameters such as the mean and standard deviation converging at this sample size to ensure reliable results. The outcomes are presented in terms of the inverse CDF of the probability of failure (P_i), denoted as $\Phi^{-1}(P_i)$, under high strain-rate loading conditions. The simulation results are illustrated in Figs. 16a and 16b, while the corresponding plots of Pi and $\Phi^{-1}(P_i)$ are shown in Figs. 15a and 15b, respectively. These graphical representations provide a comprehensive understanding of the failure probabilities and their statistical distribution, facilitating an in-depth assessment of structural reliability and post-impact reduced resilience under low velocity car crashes.

The P_f quantifies the likelihood that the pier will not perform adequately under the specified impact conditions. A P_f of 0.21 means there is a 21% chance of failure, while 0.39 indicates a 39% chance, both significant risks, with the latter showing a notably higher vulnerability.

The residual index (ζ_P) is a complementary measure that represents the remaining structural capacity of the pier after the impact, expressed as a fraction of its original capacity. For example, a ζ_P of 0.79 suggests the pier retains 79% of its initial strength post-impact, while 0.61 indicates a more substantial reduction, retaining only 61%.

These values help engineers understand not only how likely the structure is to fail but also the extent to which its load-bearing capacity is diminished after an impact. This dual insight is critical for assessing safety, planning repairs, or deciding on strengthening protocols following a low velocity collision event.

Deterministic analysis using λ is employed to assess low to moderate damage levels and to estimate the residual capacities of the impacted pier. This approach evaluates the extent of damage caused by low-velocity vehicle impacts. A representative prototype RC pier is examined to understand

Figure 14. Resulting cracks for (a) experimental and (b) FEM

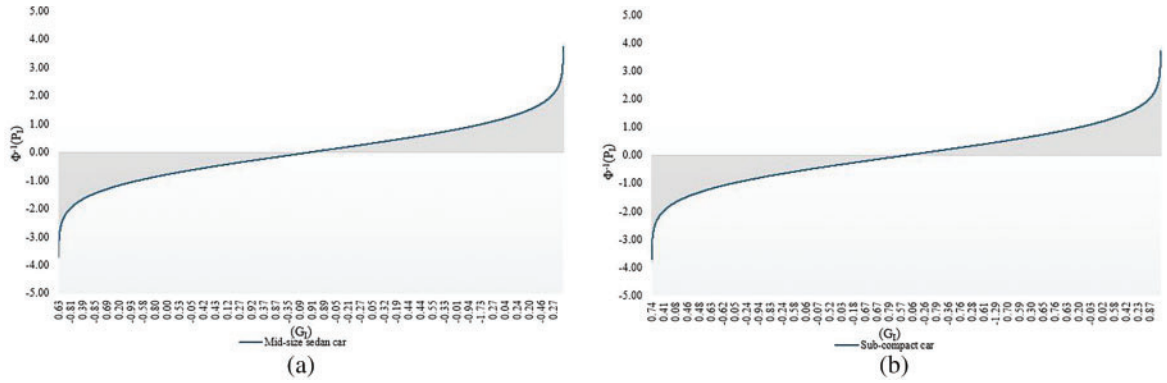

Figure 15. MC simulation impact results for (a) subcompact and (b) mid-sized sedan cars

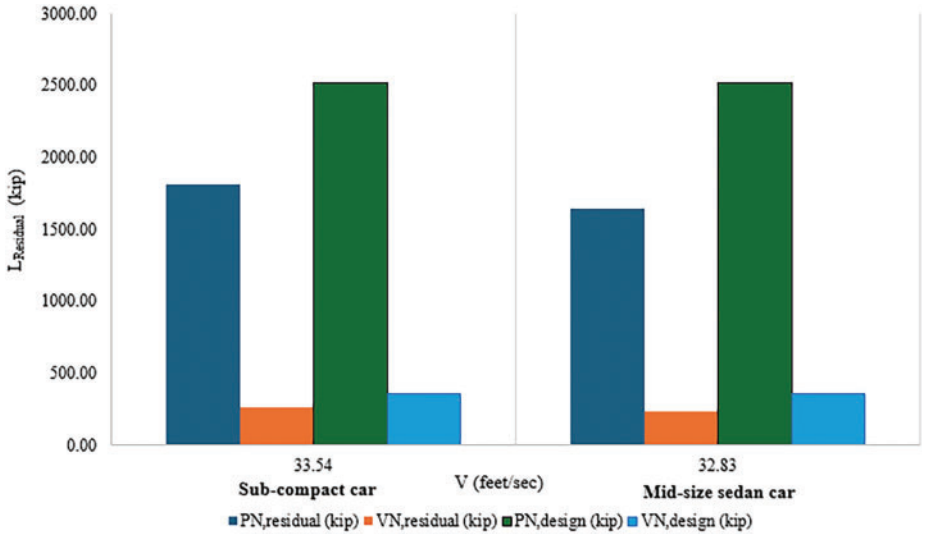

Figure 16. Residual capacities of RC pier impacted at a specific vehicle weight at specific impacting speed

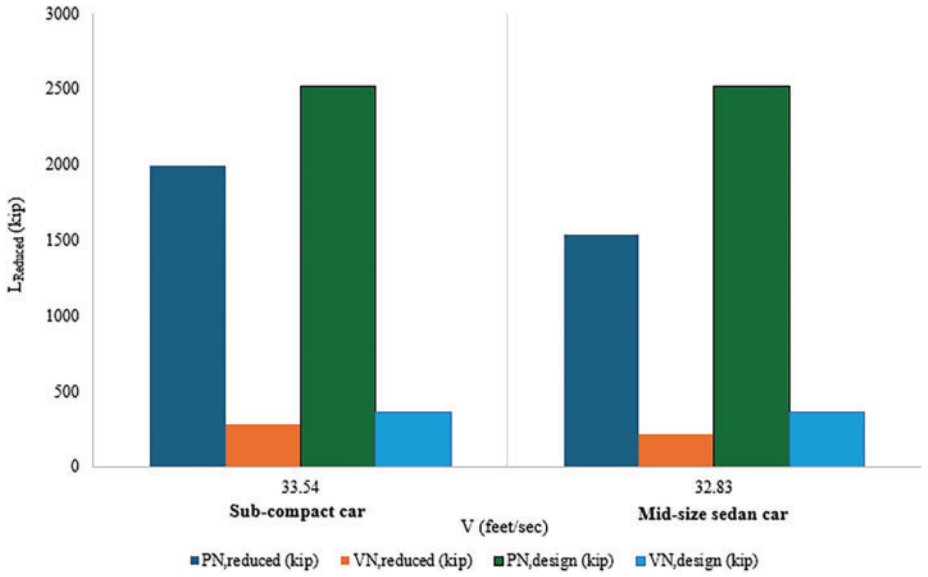

Figure 17. Residual capacities of RC pier impacted at a specific vehicle weight at specific impacting speed

its post-impact behavior, focusing on residual axial and shear capacities under specific vehicle weights and impact speeds. The resulting performance levels of the pier after impact are compared and illustrated in Fig. 16.

The probability of failure (P_f) values extracted from Figs. 15 and 16 showing 0.21 and 0.39, respectively, indicate varying levels of risk under different loading scenarios. Applying Eqs. (17) and (18), the P_f and the associated β are computed as 0.81 and 0.28. These metrics reveal a marked decline in structural reliability, emphasizing the heightened vulnerability of the system under increased impact demands. Furthermore, the ζ_P values, calculated as 0.79 and 0.61 via Eq. (19), quantify the degradation in structural performance, reflecting reduced safety margins.

The subsequent evaluation of reduced capacities through Eq. (20), with results presented in Fig. 17, provides critical insight into how impact loading compromises the load-bearing ability of the RC pier. This probabilistic assessment not only highlights key thresholds where failure becomes more probable but also underscores the importance of incorporating reliability-based approaches in design and retrofitting strategies. Ultimately, these findings advance a more nuanced understanding of structural resilience, enabling engineers to make informed, and risk-aware decisions to enhance infrastructure safety.

Determination of normalized β

From Figs. 15 and 16, the determined P_f at the respective impact conditions is determined as 0.21 and 0.39, indicating a moderate increase in failure likelihood with higher impact levels. Using Eqs. (17) and (18), the estimated P_f and the corresponding β are determined as 0.81 and 0.28, respectively. These values highlight the reduced safety margin under more severe loading, emphasizing the sensitivity of the system to variations in impact conditions. The ζ_P values, evaluated from Eq. (19), are found to be 0.79 and 0.61, further confirming the decline in reliability under increased stress levels. The corresponding reduced capacities, determined using Eq. (20), are presented in Fig. 17, showing a clear decrease in structural capacity with increasing impact intensity.

By further analyzing the results in Figs. 16 and 17, a normalized β is derived to account for variations in structural response across different crash scenarios. This normalized β\betaβ is used to calculate an overall standardized metric representing the behavior of a representative pier subjected to specific low-velocity vehicle impacts. Fig. 18 illustrates a comprehensive methodology that integrates experimental data, normalization procedures, and standardization techniques to provide a consistent and quantitative assessment of pier performance at specific strain rate impact loads. By systematically incorporating variations in impact intensity, pier properties, and observed responses, this approach enables more reliable comparisons and enhances predictive modeling for low-velocity crash scenarios, corroborating both structural design evaluation and safety assessment.

For specific low-velocity crash conditions applied to a half-sized traditional RC bridge pier, the normalized β values have been plotted against the corresponding P_f values. Using Eq. (18), a nonlinear trend of β is identified, showing an exponential relationship with P_f. This trend indicates that small increases in impact force produce progressively larger changes in the β response, reflecting the pier's nonlinear deformation and energy-absorption behavior under impact.

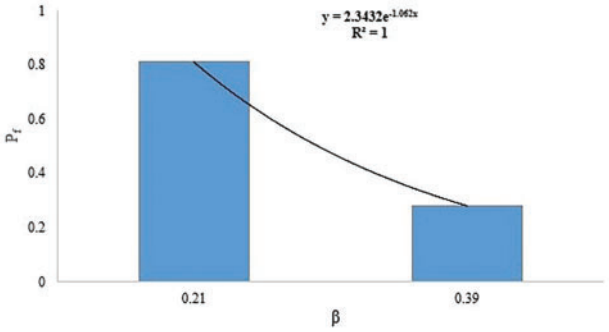

Figure 18. Normalized β and P_f

The model achieves an R^2 value of 1.0, demonstrating that the exponential relationship accurately captures the pier's response across the tested scenarios. This provides both a precise predictive tool and a meaningful physical interpretation of how low-velocity crashes influence the pier's structural behavior, where a gradual exponential decrement occurs as shown in Eq. (21)

$$P_f = 2.34 * e^{-1.062\beta} \tag{21}$$

where P_f and β are already explained.

Calibration formalism

In this study, a representative prototype RC pier is evaluated under a range of impact conditions, using vehicle weight and velocity parameters that simulate realistic collision scenarios. The objective is to assess how such impacts affect the pier's residual strength, predict its post-impact behavior, and propose a calibration process).[22,29] This deterministic analysis provides critical insights into the pier's remaining serviceability and its capacity to withstand additional loading after damage.[30] Comparative results are presented in Fig. 16, and offering a clear visual summary of the pier's performance across varying impact severities as illustrated in Table 10.

The present study investigates the impact response of a representative RC pier under realistic vehicle collision scenarios defined by weight and velocity, emphasizing residual strength and post-impact performance as shown in Table 11. Deterministic analysis captures the pier's remaining serviceability, while probabilistic evaluation predicts an 8.68% higher capacity for subcompact and a 6.86% lower capacity for mid-sized sedan impacts. The findings underscore the influence of input uncertainties and demonstrate the complementary value of deterministic and probabilistic approaches in evaluating post-impact structural resilience.

The results can be further interpreted by introducing a safety factor (η), defined as the ratio of the post-impact capacities predicted using the probabilistic framework to those obtained from the deterministic methodology. By expressing the relative capacities in this manner, η provides a direct and quantitatively robust indicator of the degree of discrepancy between the two evaluation procedures. This, in turn, facilitates a more comprehensive assessment of whether either method exhibits systematic conservativeness or permissiveness under varying impact conditions. The

Table 10. Failure evaluation

	Experimental		Deterministic		Probabilistic	
Car type	P_f	ζ_E	P_f	ζ_P	P_f	ζ_P
Subcompact	0.15	0.75	0.28	0.72	0.21	0.79
Mid-sized sedan	0.21	0.79	0.35	0.65	0.39	0.61

Table 11. Factors estimating residual capacities

	Deterministic		Probabilistic		Percent difference	
Car type	λ	ζ_D	P_f	ζ_P	Axial	Shear
Subcompact	0.28	0.72	0.21	0.79	8.68	8.68
Mid-sized sedan	0.35	0.65	0.39	0.61	6.86	6.86

formal definition of η is presented in Eq. (22), and the corresponding values derived from the dataset are compiled in Table 11.[27]

$$\eta = \frac{\zeta_P}{\zeta_D} \tag{22}$$

where η represents the calibrated safety factor, and ζ_P and ζ_D are the factors utilized to determine specific low–velocity, post-vehicle impacted residual capacities estimated, respectively, by using respective probabilistic and deterministic approaches.

Bayesian-chaotic-risk analysis

Bayesian-chaotic-risk analysis of Eq. (22) is crucial to be investigated for estimating single impact risk in terms of failure, as shown in Eq. (23)

$$P_f = \int P(y < 0|\theta)\, p(\theta|D)\, d\theta \tag{23}$$

where P_f has been explained, y is denoted as $ln(\zeta_D/\zeta_P)$, and $p(\theta|D)$ is the posterior distribution of parameters after observing crash data D and shall be estimated using Baye's theorem as shown in Eq. (24)[31]

$$p(\theta|D) = \frac{p(D)\, \mathrm{p}(\mathrm{D}|\theta)}{\mathrm{p}(\theta)} \tag{24}$$

Eq. (25) can capture epistemic uncertainty triggering limited number of crash tests, model uncertainty, measurement error, and chaotic amplification uncertainty.

Failure is shown when Eq. (25) is used, utilizing Eqs. (23) through (24)

$$g < 0 \Longleftrightarrow \eta < 1 \tag{25}$$

where η signifies calibration and equals to ζ_D/ζ_P, which is already explained in Eq. (22), and y is as shown in Eq. (23) is given by $ln(\eta)$ and equals to $ln(\zeta_D/\zeta_P)$.

Failure can be more precisely captured when η is further defined as shown in Eq. (26)

$$\eta < 0 \Longleftrightarrow \eta < 1 \tag{26}$$

Therefore, the analytical interpretation suggests that deterministic capacity remains below probabilistic capacity, indicating that safe calibration has been achieved. This condition is best understood by evaluating chaotic risk, which functions as the key diagnostic measure for identifying the potential onset of unstable and unpredictable system behavior.

This effect is conceptualized as the chaotic risk amplification factor (CRAF), a parameter that quantifies how marginal disturbances can amplify within the system and potentially trigger chaotic risk dynamics. CRAF is a metric that quantifies how much structural failure risk is increased due to chaotic effects and deep uncertainty in system behavior. It is the ratio between the failure probability obtained under chaotic, fully Bayesian calibration and the failure probability estimated using conventional or deterministic assumptions. In essence, CRAF captures the degree to which sensitive dependence on initial conditions, nonlinear interactions, and model uncertainty amplify the assessed risk of estimating η, providing a clear and meaningful indicator of how much unassessed or underestimated risk emerges when chaotic dynamics are rigorously accounted for.

In this study, this has been insightfully utilized to illustrate risk through using CRAF, which is defined in Eq. (27)

$$CRAF = \frac{Var_{chaotic}(\eta)}{Var_{gaussian}(\eta)} \tag{27}$$

where *Var* signifies *variance* of the statistical analysis of crash data, $Var_{chaotic}$ is the variance estimated using Bayesian calibration that accounts for nonlinear sensitivity, parameter uncertainty, and model-form uncertainty under low-velocity impact loading, and $Var_{gaussian}$ represents the gaussian variance from a conventional gaussian deterministic or single-model calibrated analysis.

In this specific scenario, CRAF ≈ 1, indicates the system is relatively stable to uncertainty, but the structure exhibits strong sensitivity to small variations in impact parameters.

Table 12. Conversion chart for the US customary to the equivalent SI units. SI, standard international

US customary	SI unit
1 ksi 1 psi	6.89 MPa (kN/mm^2) 0.00689 Mpa (kN/mm^2)
1 kip-in	0.113 kN-m
1 kip	4.45 kN
1 lbs	0.00445 kN
1 mph	1.61 km/hr
1 ft-lb/sec	0.00136 kN-m/sec (1.36 N-m/sec)

Discussions of Results

Deterministic analysis based on the λ approach is used to assess the extent of structural degradation in RC piers subjected to low-velocity vehicle impacts. The damage index quantifies the severity of damage by correlating it with reductions in the pier's load-carrying capacity. This approach is especially valuable for detecting low to moderate levels of damage that may not be visually obvious but can significantly compromise structural performance. By capturing indicators such as cracking, spalling, and internal stress redistribution, the λ method enables engineers to estimate residual axial and shear capacities with a reasonable degree of accuracy.

- The P_f quantifies the likelihood that a pier will not perform adequately under the specified impact conditions. A P_f of 0.21 corresponds to a 21% probability of failure, whereas a P_f of 0.39 indicates a substantially higher risk, highlighting increased vulnerability under more severe impact scenarios.
- The residual index represents the remaining structural capacity of the pier after impact, expressed as a fraction of its original strength. For example, a ζ_P of 0.79 suggests that the pier retains 79% of its initial capacity, whereas a ζ_P of 0.61 reflects a more pronounced reduction, indicating significant post-impact strength loss.
- Post-impact performance of RC bridge piers was evaluated through experimental testing and FEM simulations, considering axial compression combined with low-velocity vehicular impacts. Reliability analysis provided a probabilistic measure of post-damage safety, integrating structural performance and uncertainty.
- Despite conservative fixed-base assumptions, FEM models closely reproduced experimental deformations, effectively capturing stress concentrations at critical regions such as the pier base and foundation corners, precisely capturing the load transmittance path, which are particularly susceptible to spalling and splitting.
- Simulations identified peak stress concentrations at the pier base–foundation interface under sub-compact and mid-sized sedan impacts. Predicted crack initiation zones closely matched experimental observations, with deviations limited to within 5%, demonstrating the model's predictive accuracy.
- Comparison with published data confirmed strong agreement in deformation patterns, stress magnitudes, and crack initiation locations, which accurately corroborates load transmittance path. This alignment further validated the slightly conservative FEM model, reinforcing confidence in its predictive reliability.

Conclusions

RC bridge piers, often positioned in exposed locations such as highway medians or bridge approaches, are especially susceptible to vehicular collisions due to their slender geometry and limited lateral resistance. Despite their critical structural role, the dynamic impact response and damage mechanisms of RC piers under sudden vehicle loads remain inadequately understood. Such knowledge gaps warrant the development of effective design strategies and protective measures aimed at improving pier resilience and ensuring overall structural safety protocol following the specific impact events.

To address this limitation, the present study employs an integrated approach that combines analytical modeling, FEM simulations, and experimental validation. This comprehensive framework enables the investigation of both the immediate impact response and the subsequent residual capacity of RC piers after collision. By correlating numerical predictions with empirical data, the study provides deeper insights into damage progression, energy dissipation mechanisms, and post-impact load-bearing behavior. Ultimately, the outcomes contribute to more accurate performance prediction models and inform the design of more robust RC piers capable of withstanding realistic vehicular impact scenarios.

(1) Performance-based studies of the impacted pier are investigated and presented for short-duration impacts to capture the low to cosmetic damages of the representative piers.
(2) This research is an attempt to investigate the material requirements for enhancing resistance. Additionally, this instills an insightful idea and realistic correlation between experimental and numerical simulations.[32,33]
(3) Simulations accurately identify critical damage in RC piers and foundations under low-velocity impacts.

Using a conservative resistance–reduction method, post-impact failure is probabilistically assessed, providing insights into material behavior and impact performance for future calibration without destructive testing.

(4) However, before making cognitive conclusions regarding cosmetic damage and developing methods for re-strengthening and enhancing resilience, it is recommended to conduct high-precision experimental studies encompassing a variety of geometries, material properties, and impact scenarios.

(5) The validated FEM framework accurately predicted residual capacity and observed damage patterns, demonstrating its effectiveness as a reliable predictive tool for evaluating the post-impact resilience of RC bridge piers. By closely replicating experimental behavior and capturing key nonlinear damage mechanisms under impact loading, the model provides practicing structural engineers with a robust methodology for assessing probabilistic post-damage performance and making informed structural safety decisions regarding the resilience and reliability of damaged bridge infrastructure.

(6) Such dual insights, quantifying both residual capacity and failure probability, seems essential for informed decision-making regarding pier safety, enabling engineers to accurately evaluate structural integrity, prioritize interventions, and optimize resource allocation. By integrating deterministic capacity assessment with probabilistic risk evaluation, the study provides a comprehensive basis for planning repairs, designing strengthening measures, and ensuring the continued safety and serviceability of bridge piers following a specific collision event.

(7) The final intuitive explanation is that P_f represents the average probability of failure, weighted by how plausible each competing model is. Rather than relying on a single "best" model, it incorporates uncertainty across all candidate models, giving greater influence to those better supported by the evidence. Thus, P_f provides the most complete probabilistic statement of structural risk under Bayesian chaotic calibration, integrating both model and parameter uncertainty into a unified and balanced assessment of failure risk.

(8) Practically, the study complies with the fact that columns with higher CRAF values may appear safe under mean-value analysis but show elevated failure probability when uncertainty is rigorously propagated. This affects predictions of local damage extent, global instability risk, and post-impact residual strength. In design and assessment, a high CRAF signals the need for conservative safety margins, impact-resistant detailing (e.g., confinement reinforcement), or strengthening measures, while a low CRAF suggests the column's response is relatively stable and less vulnerable to uncertainty assessment.

In summary, this study provides a critical step toward enhancing the safety and longevity of RC bridge piers exposed to vehicle impacts, combining rigorous simulation and validation efforts with practical recommendations for future research and infrastructure resilience.

Table 12 provides a comprehensive conversion chart for accurately translating measurements between U.S. Customary Units and the Standard International System of Units. As a key reference, the chart ensures consistency and precision in unit conversions, supporting uniform calculations and analysis throughout the article. By offering reliable conversion factors, it facilitates seamless cross-referencing and comparison of data across different measurement systems, thereby enhancing the clarity and applicability of the presented information.

Competing Interests

The authors declare that there are no competing interests.

Data Availability Statement

Some or all data, models, or code that support the findings of this study are available from the corresponding author upon reasonable request.

Funding

This research is funded by the Department of Civil and Environmental Engineering, Utah State University, Logan, Utah 84322, USA.

References

[1] Sharma H, Gardoni P, Hurlebaus S. Performance-Based probabilistic capacity models and fragility estimates for RC columns subject to vehicle collision. *Comput-Aid Civil Infrast Eng*. 2015;30(7):555–569. doi:10.1111/mice.12135.

[2] El-Tawil S, Severino E, Fonseca P. Vehicle collision with bridge piers. *J Bridge Eng*. 2005;10(3):345–353. doi:10.1061/(asce)1084-0702(2005)10:3(345).

[3] Thilakarathna HMI, Thambiratnam DP, Dhanasekar M, Perera N. Numerical simulation of axially loaded concrete columns under transverse impact and vulnerability assessment. *Int J Impact Eng, Pergamon*. 2010;37(11):1100–1112. doi:10.1016/j.ijimpeng.2010.06.003.

[4] Roy S. Precision assessment of reinforced concrete RC bridge pier resilience under high-velocity vehicle impact using an energy-based analytical model. *Int J Bridge Eng, ManagRes, BER*. 2025a;2(3). Publication date: July 10, 2025. doi:10.70465/ber.v2i3.40.

[5] Roy S. Stochastic modeling of vehicle impact on reinforced concrete bridge piers: assessment of structural reliability and resilience. *Recent Prog Sci*. 2025b;2(1):013. doi:10.70462/rps.2025.2.013.

[6] Ebrahimpour A, Earles BE, Maskey S, Tangarife M, Sorensen AD. *Seismic Performance of Columns with Grouted Couplers in Idaho Accelerated Bridge Construction Applications*. Idaho: Transportation Dept.

[7] Tazarv M, Saiidi MS. Seismic design of bridge columns incorporating mechanical bar splices in plastic hinge

regions. *Eng Struct, Elsevier*. 2016;124(2):507–520. doi:10.1016/j.engstruct.2016.06.041.
[8] Zhou D, Li R, Wang J, Guo C. Study on impact behavior and impact force of bridge pier subjected to vehicle collision. *Shock Vibrat*. 2017;2017(18):1–12. doi:10.1155/2017/7085392.
[9] Roy, S. Sustainability and resiliency investigation of grouted coupler embedded in RC ABC bridge pier at vehicle impact. *Eng Appl Sci*. 2024;9:14–33.
[10] Furlong RW, Ferguson PM, Ma JS. *Shear and Anchorage Study of Reinforcement in Inverted T-Beam Bent Cap Girders*. Project No. 3-5-68-113. Austin, TX: Center for Highway Research, Univ. of Texas at Austin; 1971.
[11] Ameli MJ, Pantelides CP. Seismic analysis of precast concrete bridge columns connected with grouted splice sleeve connectors. *J Struct Eng, American Soc Civil Eng*. 2017;143(2):4016176.
[12] Sun X, Bi Y, Zhou R, et al. *Experimental Study on the Damage of Bridge Pier under the Impact of Rockfall*. 2021.
[13] Li RW, Zhou DY, Wu H. Experimental and numerical study on impact resistance of RC bridge piers under lateral impact loading. *Eng Fail Anal, Pergamon*. 2020b;109(1):104319. doi:10.1016/j.engfailanal.2019.104319.
[14] Feyerabend M. *Hard Transverse Impacts on Steel Beams and Reinforced Concrete Beams*. Germany: University of Karlsruhe (TH); 1988.
[15] Li RW, Wu H, Yang QT, Wang DF. Vehicular impact resistance of seismic designed RC bridge piers. *Eng Struc, Elsevier*. 2020a;220(8):111015. doi:10.1016/j.engstruct.2020.111015.
[16] Jack. "How Much Does A Car Weigh?" *Auto Shop Accessories*; 2019. https://www.drivinggeeks.com/average-weight-car/. January 21, 2022.
[17] Roy S. Reliability analysis and uncertainty evaluation for assessing low velocity car impacted cosmetic damage of prototyped RC bridge pier. *J Ins-Civil Eng*. September 29, 2024;7(1):1. doi:10.18282/ice.v7i1.623.
[18] Standard AA. *Building Code Requirements for Structural Concrete (ACI 318-11)*. American Concrete Institute; 2011 August. Vol. 680, 681.
[19] American Society of Civil Engineers. *Minimum Design Loads and Associated Criteria for Buildings and Other Structures (ASCE/SEI 7-16)*. American Society of Civil Engineers; 2017. doi:10.1061/9780784414248.
[20] AASHTO. *Guide Specifications for LRFD Seismic Bridge Design*. 2nd Edition. Washington, DC: American Association of State Highway and Transportation Officials; 2011.
[21] AASHTO, M. *145–91. Classification of Soils and Soil-Aggregate Mixtures for Highway Construction Purposes*. Washington, DC: AASHTO DESIGNATION, American Association of State Highway and Transportation Officials; 1993, 122–126.
[22] Wiacek C, Nagabhushana V, Rockwell T, Summers S, Zhao L, Collins LA. Evaluation of frontal crash stiffness measures from the US New car assessment program. *ESV Conference*, Seoul, South Korea.
[23] Ayyub BM, McCuen RH. *Probability, statistics, and reliability for engineers and scientists*. CRC press; 2025.
[24] Der Kiureghian A. Analysis of structural reliability under parameter uncertainties. *Probab Eng Mech*. 2008;23(4):351–358. doi:10.1016/j.probengmech.2007.10.011.
[25] Nowak AS, Collins KR. *Reliability of Structures*. 2nd ed. CRC Press; 2012.
[26] Seegmiller LW. *Utah Commercial Motor Vehicle Weigh-in-Motion Data Analysis and Calibration Methodology*. Brigham Young University; 2006.
[27] Hwang E, Nowak AS. Simulation of dynamic load for bridges. *J Struct Eng*. 1991;117(5):1413–1434. doi:10.1061/(asce)0733-9445(1991)117:5(1413).
[28] Roy S, Majumdar BB. Predictive assessment of crack behavior in RC bridge piers under vehicle impact: a reliability and resilience-based approach. *Innov Infrastruct Solut*. 2025;10(12):586.
[29] Ameli MJ, Brown DN, Parks JE, Pantelides CP. Seismic column-to-footing connections using grouted splice sleeves. *ACI Struct J, American Conc Inst*. 2016;113(5):1021–1030. doi:10.14359/51688755.
[30] Girão Coelho AM, Simão PD, Bijlaard FSK. Guidance for the design of spliced columns. *J Struct Eng, American Soc Civil Eng*. 2012;138(9):1079–1088. doi:10.1061/(asce)st.1943-541x.0000546.
[31] Navidi WC. *Statistics for Engineers and Scientists*. vol. 2. New York: McGraw-Hill; 2006. ISBN 978-0-07-340133-1.
[32] Jacob GC, Fellers JF, Starbuck JM, Simunovic S. Crashworthiness of automotive composite material systems. *J Appl Polym Sci* 2004;92(5):3218–3225. doi:10.1002/app.20336.
[33] Pantelides CP, Ameli MJ, Parks JE, Brown DN. *Seismic Evaluation of Grouted Splice Sleeve Connections for Precast Rc Bridge Piers in Accelerated Bridge Construction (ABC) (Report No. UT-14.09)*. Utah Department of Transportation, Research Division; 2014.